Computers and Geotechnics 110 (2019) 199–210

Contents lists available at ScienceDirect

Computers and Geotechnics

journal homepage: www.elsevier.com/locate/compgeo

Research Paper

Effect of soil variability on bearing capacity accounting for non-stationary characteristics of undrained shear strength

Yongxin Wu[a], Xuhui Zhou[a], Yufeng Gao[a,*], Limin Zhang[b], Jun Yang[c]

[a] Key Laboratory of Ministry of Education for Geomechanics and Embankment Engineering, Hohai University, No. 1, Xikang Road, Nanjing 210098, China
[b] Department of Civil and Environmental Engineering, The Hong Kong University of Science and Technology, Clear Water Bay, Hong Kong
[c] Department of Civil Engineering, The University of Hong Kong, Pokfulam Road, Hong Kong

ARTICLE INFO

Keywords:
Bearing capacity
Random field
Spatial variability
Non-stationary
Undrained shear strength
Monte Carlo simulation

ABSTRACT

The objective of this paper is to investigate the bearing capacity of spatially varying soil in the presence of non-stationary feature of undrained shear strength. Firstly, undrained shear strength is modeled by a non-stationary random field. In this model, the mean of undrained shear strength is non-zero at the ground surface and linearly increases with depth, while the coefficient of variation (COV) of undrained shear strength keeps constant. Based on this non-stationarity, an algorithm is proposed to produce the corresponding random field. Then, Monte Carlo Simulations are carried out to evaluate the statistical characteristics of the resulted bearing capacity, followed by a detailed discussion on the effects of COV, strength gradient parameter, distribution type, and vertical auto-correlation length. At last, two computation schemes that enable the prediction of statistical characteristics (e.g., mean, standard deviation, and cumulative probability function) of bearing capacity in non-stationary random fields utilizing results from a stationary one are proposed, and demonstrated through numerical examples.

1. Introduction

It has been widely recognized that soils sometimes show considerable spatial variability, resulting in significant uncertainties in the estimation of soil parameters. The uncertainties are mainly due to the following aspects: inherent soil variability, measurement errors, and model transformation uncertainties [27]. Random field theory can be adopted by introducing suitable correlation models to account for the inherent soil variability, i.e. the variation of soil properties from one point to another in space due to different depositional conditions and different loading histories.

The past two decades have witnessed the growing interest of studying the potential impacts of soil variability on the geotechnical performance. Such a research covers a wide range of geotechnical problems, such as the bearing capacity of foundations [12,13,9,29,32,33,3,21,23], settlements of foundations [8,10,20], the stability of slopes [1,14,15,33,4,39,18,19,38], and so on. The past studies have clearly shown the importance of spatial variability of soil properties for geotechnical designs. In general, considering the spatial variability leads to a rational and economical design of foundations [31,6]. Furthermore, some realistic failure modes, such as the non-symmetric failure mode [12,29], which could not be observed under the assumption of homogeneous soils, would be easily identified by taking the spatial variability of soil properties into account.

In the presence of soil variability, various probabilistic methods have been developed for predicting the reliability of geotechnical structures. These include first-order second-moment (FOSM) method, first-order reliability method (FORM), response surface method, and Monte Carlo Simulation (MCS). Albeit computationally expensive, MCS is often adopted in the reliability analysis due to its high accuracy. That is why MCS has long been used to benchmark other approaches. Recently, MCS implemented through random finite-element method (RFEM) or non-intrusive stochastic analysis that integrates a commercial finite difference method and the random field theory, has become a popular approach to study the influence of soil variability on geotechnical performances. In view of the advantages, this study will employ MCS to investigate the effect of spatial variability of undrained shear strength on bearing capacity of a shallow foundation, which is a classical geotechnical subject. As mentioned previously, the topic has attracted considerable attentions, and it is reported that the bearing capacity of a footing can be overestimated without accounting for the inherent random heterogeneity of soils [13].

The stationary random field model has been widely used to describe the spatial variability of soil parameters. However, it is well known that soil parameters often exhibit non-stationary characteristics. Lumb [26] pointed out two typical non-stationary types of soil properties: (a) mean

* Corresponding author.
E-mail addresses: yfgao66@163.com (Y. Gao), cezhangl@ust.hk (L. Zhang), junyang@hku.hk (J. Yang).

https://doi.org/10.1016/j.compgeo.2019.02.003
Received 3 December 2018; Received in revised form 4 February 2019; Accepted 4 February 2019
Available online 22 February 2019
0266-352X/ © 2019 Elsevier Ltd. All rights reserved.

of soil parameter linearly increases with depth while its standard deviation keeps constant; (b) both mean and standard deviation of soil parameter increase with depth while its COV keeps constant. In the case of type (a), a stochastic parameter is usually divided into a trend function and a fluctuating component, and the fluctuating component can be considered to be a zero-mean stationary random field. The reliability analysis of geotechnical problems involving type (a) spatial variability has been well documented in the literature, such as Sivakumar Babu et al. [32,33]. The spatial variability of type (b) is always confined to the undrained shear strength because it depends on effective stress of soil [26]. In the framework of probabilistic geotechnical analysis, only a few recent works considered the non-stationary characteristics of soil properties, for instance, Li et al. [22,21], Griffiths et al. [16], Muller et al. [25], and Zhu et al. [38]. In this study, the non-stationary random field model, whose mean value increases linearly with depth while the COV remains constant as applied by Zhu et al. [38], will be adopted to investigate the influence of spatial variability of undrained shear strength on the bearing capacity of a shallow foundation.

When investigating the effects of spatial variability of soil properties on the bearing capacity, it is generally assumed (but not always) that the undrained shear strength follows the lognormal distribution. However, based on several studies reported in the literature, undrained shear strength can follow different probability distribution functions (PDF's) for different types of soils and sites [29,2,35]. According to Popescu et al. [29], the distribution type employed to define the soil's shear strength can have a considerable influence on the resulted bearing capacity. As a result, this study will consider three different types of distributions, e.g., Lognormal, Gamma and Beta.

The remainder of this paper is organized as follows. In the following section, the method to simulate non-Gaussian non-stationary random field based on the spectral representation method is proposed. Then, the finite element model for analysis of the bearing capacity of a shallow foundation is presented. In the finite element model, the random field of the bearing capacity is simulated by the proposed method. Finally, the results of the bearing capacity computed by MCS are discussed, and the effects of non-stationary characteristics and different distribution types of the undrained shear strength are illustrated.

2. Simulation of non-Gaussian non-stationary fields

In the stochastic analysis by MCS, a continuous-parameter random field must be discretized into random variables to be implementable by numerical method. In this regard, several methods have been developed, such as the midpoint method [5], the local average subdivision (LAS) method [11], Turning bands methods (TBM) [24], the KL expansion [28] and the spectral representation method (SRM) [37,30]. Fenton [7] systematically investigated the characteristics of three common random field generators (i.e. SRM, TBM and LAS), and gave a number of useful and helpful guidelines and suggestions to choose the algorithm in the application. Then, Stefanou and Papadrakakis [34] proved that the SRM exhibits good features in converging to the target autocorrelation function in the simulation of random process. In this paper, the SRM is considered. The SRM is firstly proposed by Yaglom [37], then developed by Popescu et al. [30] to simulate non-Gaussian random field. Just recently, Wu et al. [36] developed the SRM proposed by Popescu et al. [30] and provided an efficient method to simulate multi-dimensional stationary non-Gaussian random fields by introducing a highly efficient iterative scheme. For simplicity, the improved SRM method proposed by Wu et al. [36] will be extended herein to simulate non-stationary non-Gaussian random field, as detailed below. For more details about the feature of SRM, the paper given by by Wu et al. [36] can be referred.

Consider a 2D homogeneous non-Gaussian non-stationary random field $y(x, z)$, whose mean value and standard deviation increase linearly, but with a constant COV. Generally, $y(x, z)$ can be standardized by:

$$\bar{y}(x, z) = (y(x, z) - \mu_z)/\sigma_z \tag{1}$$

where $\bar{y}(x, z)$ is the standard non-Gaussian random field with zero mean value and unit variance, μ_z and σ_z are respectively the corresponding mean value and standard deviation of the prescribed random field at the depth z. It is clear that the random field $\bar{y}(x, z)$ is stationary subjected to an autocorrelation function $\rho_{NG}(\xi_x, \xi_z)$. Mathematically, $\bar{y}(x, z)$ can be mapped from a standard Gaussian random field $\bar{g}(x, z)$ (named as underlying Gaussian random field) through the nonlinear memoryless transformation [17]:

$$\bar{y}(x, z) = F_{\bar{y}}^{-1}[\Phi(\bar{g}(x, z))] \tag{2}$$

where $\Phi(\cdot)$ is the standard unit Gaussian cumulative probability function (CDF) and $F_{\bar{y}}(\cdot)$ is the marginal non-Gaussian CDF of $\bar{y}(x, z)$, with inverse function $F_{\bar{y}}^{-1}(\cdot)$.

The SRM can be utilized to simulate the (standard) underlying Gaussian random field [36]:

$$\bar{g}(x, z) = \sum_{l_1=0}^{N_1-1} \sum_{l_2=0}^{N_2-1} \sqrt{S_G\left(\kappa_{xl_1}, \kappa_{zl_2}\right) \Delta\kappa_x \Delta\kappa_z} \left[\cos\left(\kappa_{xl_1} x + \kappa_{zl_2} z + \phi_{l_1 l_2}^1\right) + \cos\left(\kappa_{xl_1} x - \kappa_{zl_2} z + \phi_{l_1 l_2}^2\right)\right] \tag{3}$$

where

$$\kappa_{xl_i} = l_{1i}\Delta\kappa_x,\ l_{1i} = 0,1,\ldots,N_1 - 1 \tag{4}$$

$$\kappa_{zl_i} = l_{2i}\Delta\kappa_z,\ l_{2i} = 0,1,\ldots,N_2 - 1 \tag{5}$$

$$\Delta\kappa_x = \kappa_{xu}/N_1,\ \Delta\kappa_z = \kappa_{zu}/N_2 \tag{6}$$

and $\Delta\kappa_x$ and $\Delta\kappa_z$ are the discretization steps in the wave number domain along horizontal direction and vertical direction, respectively; and κ_{xu} and $\kappa_{zu}$are the corresponding upper cut-off wave numbers. $\phi_{l_1 l_2}^1$ and $\phi_{l_1 l_2}^2$ are two sets of $N_1 N_2$ independent random phase angles uniformly distributed over the interval $[0, 2\pi]$. $S_G(\kappa_x, \kappa_z)$ is the target Gaussian power spectral density (PSD) function, which can be obtained from the Gaussian autocorrelation function $\rho_G(\xi_x, \xi_z)$ through the Wiener-Khintchine transform:

$$S_G(\kappa_x, \kappa_z) = \frac{1}{(2\pi)^2} \int_{-\infty}^{+\infty} \int_{-\infty}^{+\infty} \rho_G(\xi_x, \xi_z) e^{-i(\kappa_x \xi_x + \kappa_z \xi_z)} \mathrm{d}\xi_x \mathrm{d}\xi_z \tag{7}$$

where ξ_x and ξ_z are the distances in horizontal and vertical directions, respectively.

According to the central limit theorem, the random fields generated by Eq. (3) are asymptotically Gaussian as N_1 and N_2 simultaneously approach infinity.

As the transformation shown in Eq. (2) is nonlinear, the Gaussian autocorrelation function $\rho_G(\xi_x, \xi_z)$ utilized to simulate the underlying Gaussian random field is not equal to the non-Gaussian autocorrelation function $\rho_{NG}(\xi_x, \xi_z)$. According to the non-Gaussian translation theory, the relationship between them can be expressed as:

$$\rho_{NG}(\xi_x, \xi_z) = \int_{-\infty}^{+\infty} \int_{-\infty}^{+\infty} F_{\bar{y}}^{-1}[\Phi(g_1)] F_{\bar{y}}^{-1}[\Phi(g_2)] \phi[g_1, g_2; \rho_G(\xi_x, \xi_z)] \mathrm{d}g_1 \mathrm{d}g_2 \tag{8}$$

where $\phi[g_1, g_2; \rho_G(\xi_x, \xi_z)]$ is the joint Gaussian probability density function (PDF) of underlying normalized autocorrelation functions $\rho_G(\xi_x, \xi_z)$.

Prior to the simulation of the underlying Gaussian random field by Eq. (3), the underlying Gaussian PSD function $S_G(\kappa_x, \kappa_z)$ should be determined. The abovementioned transformation is always possible to use in the "forward" direction, but is not always possible in the "inverse" direction. It means, given an arbitrary non-Gaussian PSD function, it is not always possible to find the exact underlying Gaussian PSD function. If the "inverse" case is not solvable, the pair of target non-Gaussian PSD function and prescribed marginal non-Gaussian CDF is considered to be "incompatible". However, in the "incompatible" cases,

there is still a strong desire to find a "compatible" underlying Gaussian PSD function, whose corresponding non-Gaussian PSD function resembles, as closely as possible, the prescribed non-Gaussian PSD function. For this purpose, a sample-free iterative scheme was proposed by [36]. The details of the sample-free iterative scheme are shown in Appendix A.

Once the underlying Gaussian PSD function $S_G(\kappa_x, \kappa_z)$ is determined, the standard underlying Gaussian random field $\bar{g}(x, z)$ can be readily generated by Eq. (3), and mapped to the standard non-Gaussian random field $\bar{y}(x, z)$ through Eq. (2). As a result, the desired non-Gaussian non-stationary random field $y(x, z)$ is obtained by

$$y(x, z) = \bar{y}(x, z)\sigma_z + \mu_z \tag{9}$$

3. Description of finite element and random field models

In this study, a plane strain finite element analysis is performed by using *ABAQUS* 6.11. The soil is modeled by a linear-elastic perfectly plastic stress-strain law with Tresca failure criterion. The strip footing is considered to be rigid and has a rough interface with the foundation soil. An increasing pressure is applied to the strip footing, and the bearing capacity failure of the footing is taken to have occurred when the applied load leveled out within quite strict tolerances [13]. The bearing capacity is the final force divided by the footing area.

The finite element model is 15 m in width and 10 m in depth, as shown in Fig. 1. The model consists of 2400 elements, with 60 columns and 40 rows, and 4-node reduced integration element with the size of 0.25 m * 0.25 m. The standard boundary conditions, i.e., roller in vertical sides and fixed in the bottom, are applied to the model.

The soil model contains three parameters, i.e. Young's modulus (E), Poisson's ratio (γ) and the undrained shear strength (c_u). In the finite element analysis, Young's modulus (E) and Poisson's ratio (γ) are simply held constant as the bearing capacity is not sensitive to these parameters [12], while the undrained shear strength (c_u) is considered as a stochastic parameter modeled by a random field. The Young's modulus is 20 MPa. The Poisson ratio is set to be 0.49 to model the undrained behavior of no volume change as well as to ensure numerical stability.

The simulation method presented in above section is applied to generate the samples of non-stationary random fields of c_u. The mean value of c_u at the depth $z = 0$ (i.e., the ground surface), $u_{c_u(z=0)}$, is set to be 40 kPa. The mean value of undrained shear strength u_{c_u} linearly increases with depth, but the COV of c_u keeps constant, i.e. 0.1, 0.3, and 0.5 in this study. The dimensionless strength gradient parameter M, defining the increasing rate of the mean value of undrained shear strength, is given as:

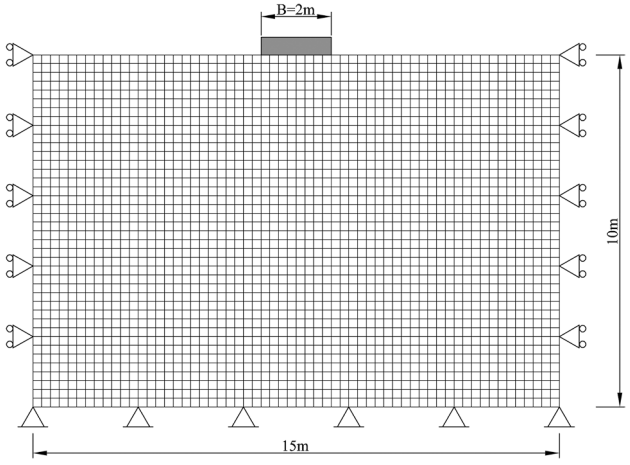

Fig. 1. FEM model of the shallow foundation.

Table 1
Summary of undrained shear strength properties.

Soil property	Symbol	Value/Range
The mean of undrained shear strength at ground surface	$u_{c_u(z=0)}$	40 (kPa)
Coefficient of variation	COV	0.1; 0.3; 0.5
The strength gradient parameter	M	0; 0.5; 1.0; 1.5
The normalized horizontal scale of fluctuation	δ_h	5
The normalized vertical scale of fluctuation	δ_v	1, 2.5, 5

Table 2
Three standard non-Gaussian distributions considered in the numerical example.

Distribution	PDF	Parameters
Lognormal	$f(x) = \frac{1}{\sqrt{2\pi}\sigma_N \bar{x}} \exp[-\frac{(\ln \bar{x} - \mu_N)^2}{2\sigma_N^2}]$ $\sigma_N^2 = \ln(1 + \frac{\sigma^2}{\bar{\mu}^2})$, $\mu_N = \ln \bar{\mu} - \frac{\sigma_N^2}{2}$, $\bar{x} = x - \bar{\mu}$	$\bar{\mu} = 2$ $\sigma = 1$
Gamma	$f(x) = \frac{1}{\Gamma(k)\theta^k} x^{k-1} e^{-\frac{x}{\theta}}$ * $x = (\bar{x} - k\theta)/\sqrt{k\theta^2}$, $x > -\sqrt{k}$	$k = 4$ $\theta = 1$
Beta	$f(x) = \frac{\Gamma(C+D)}{\Gamma(C)\Gamma(D)(B-A)^{C+D-1}} (x - A)^{C-1}(B - x)^{D-1}$ $A < x < B$	$A = -2$ $B = 3$ $C = 2$ $D = 3$

* $\Gamma(\bullet)$ is the Gamma function.

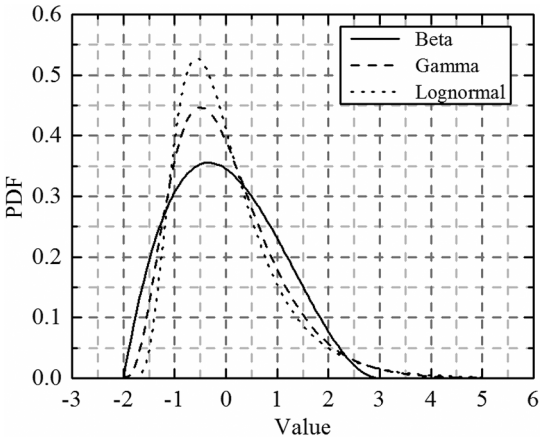

Fig. 2. The PDFs of the three standard non-Gaussian distributions with zero mean and unit variance.

$$M = \frac{u_{c_u(z=H)} - u_{c_u(z=0)}}{u_{c_u(z=0)}} \tag{10}$$

where $u_{c_u(z=H)}$ is the mean value of c_u at the bottom of the model, and H is the depth of the foundation soil, which is 10 m in the present study. The dimensionless strength gradient parameter M is set to be 0, 0.5, 1.0 and 1.5, respectively, where $M = 0$ means the random field is stationary.

A squared exponential 2-D autocorrelation function is adopted to define the spatial variability of the random field of c_u as follows:

$$\rho(\xi_h, \xi_v) = \exp(-[(\xi_h/l_h)^2 + (\xi_v/l_v)^2]) \tag{11}$$

where ξ_h and ξ_v are the lag distances between any two positions in horizontal and vertical directions, respectively; and l_h and l_v are the autocorrelation lengths defining the decay rates in the horizontal and vertical directions, respectively. Due to the nature of the stochastic process of soils, the bearing capacity is more probabilistically sensitive to l_v than to l_h [21]. To simplify the finite element analysis, this study considers a constant l_h = 10 m, and three different values of l_v = 2 m,

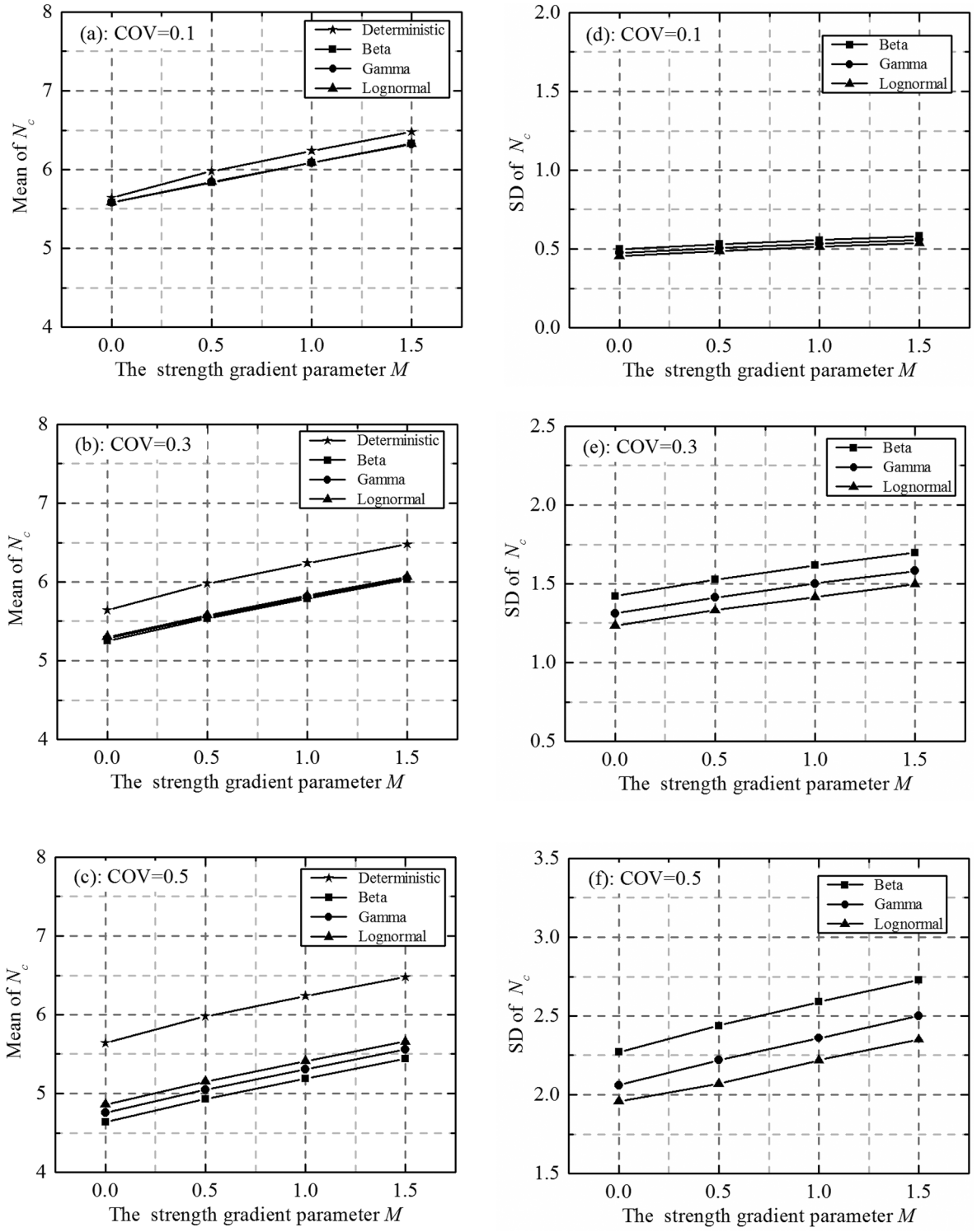

Fig. 3. The mean and standard deviation of the bearing capacity for $\delta_v = 1$. (a–c): mean value; (d–f): standard deviation.

5 m, and 10 m. To reflect the effect of geometric parameter of strip footing, the correlation lengths are normalized into dimensionless values by the width of strip footing B, resulting in normalized scales of fluctuation δ_h and δ_v. In all, the parameters involved in the simulation of non-stationary random field of c_u are summarized in Table.1.

To investigate the effect of distribution type of c_u on bearing capacity, three types of distributions are considered, i.e. Lognormal distribution, Beta distribution and Gamma distribution. The details of three standard distributions considered in this paper are given in Table.2, and the PDFs of them are plotted in Fig. 2.

Based on the coordinate of elements in the finite element models, a series of realizations of the random fields of c_u are generated by the proposed simulation method.

4. Analysis of simulation results

Extensive MCS analyses using the finite element model were conducted to evaluate the strip footing bearing capacity with both

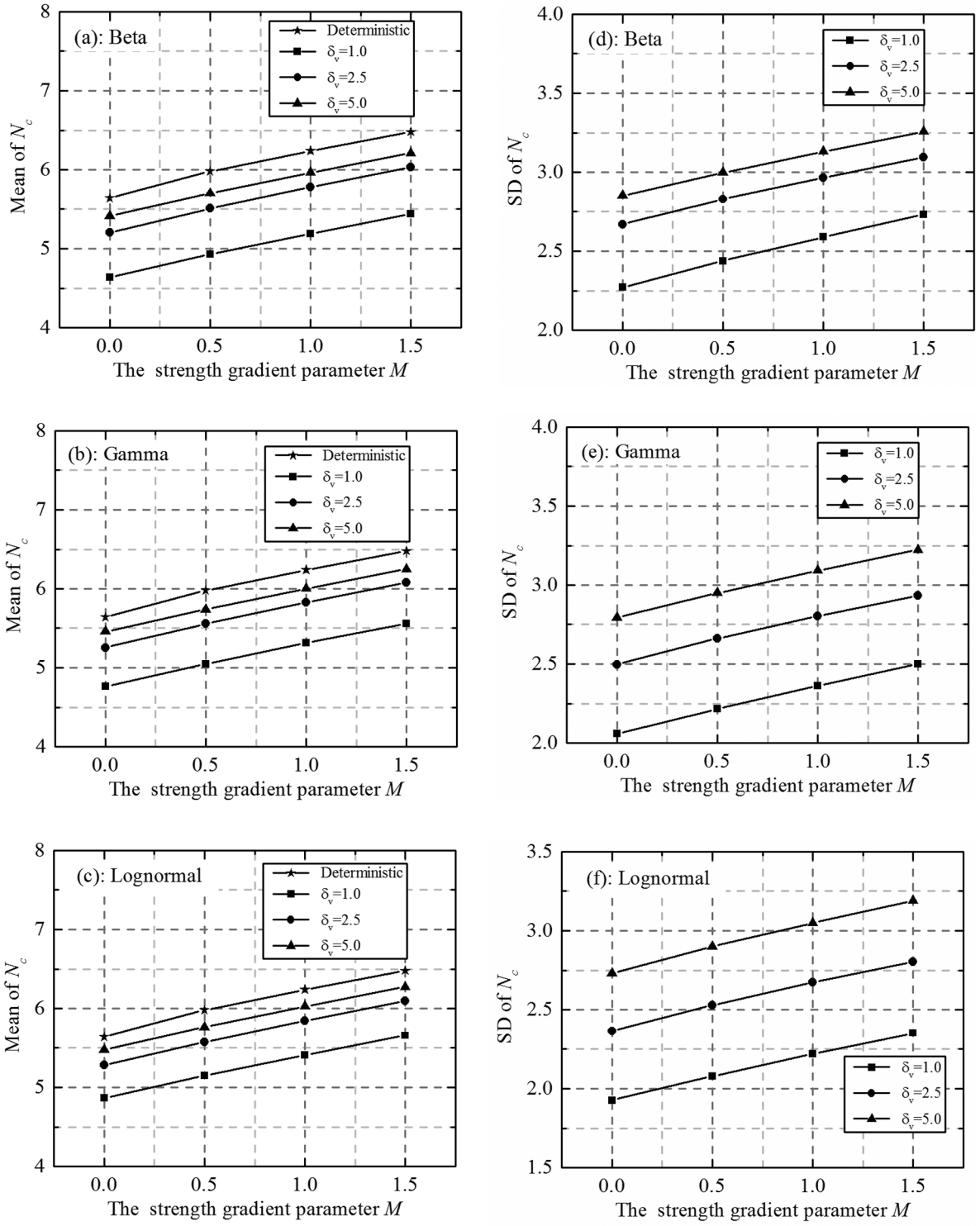

Fig. 4. The mean and standard deviation (SD) of the bearing capacity for different cases of vertical autocorrelation length with COV = 0.5. (a–c): $\delta_v = 1$; (d–f): $\delta_v = 5$.

stationary and non-stationary spatially varying foundation soils. In the framework of MCS, realizations of the random fields of c_u were recalled by a batch program to compute deterministically the bearing capacity on each of them. At last, the bearing capacities for all realizations were retrieved for statistical evaluation. In this study, 1000 simulations have been performed for each type of random fields. It is worth noting that rather than dealing with the actual bearing capacity, this study focuses on the dimensionless bearing capacity factor defined by:

$$N_{ci} = \frac{q_{fi}}{u_{c_u(z=0)}} \tag{12}$$

where q_{fi} is the bearing capacity computed for the ith realization and $u_{c_u(z=0)}$ is the mean c_u on the ground surface.

4.1. The first two statistical moments of bearing capacity

Based on the MCS results, firstly, the mean and standard deviation of bearing capacity are studied, and then the effects of COV, the

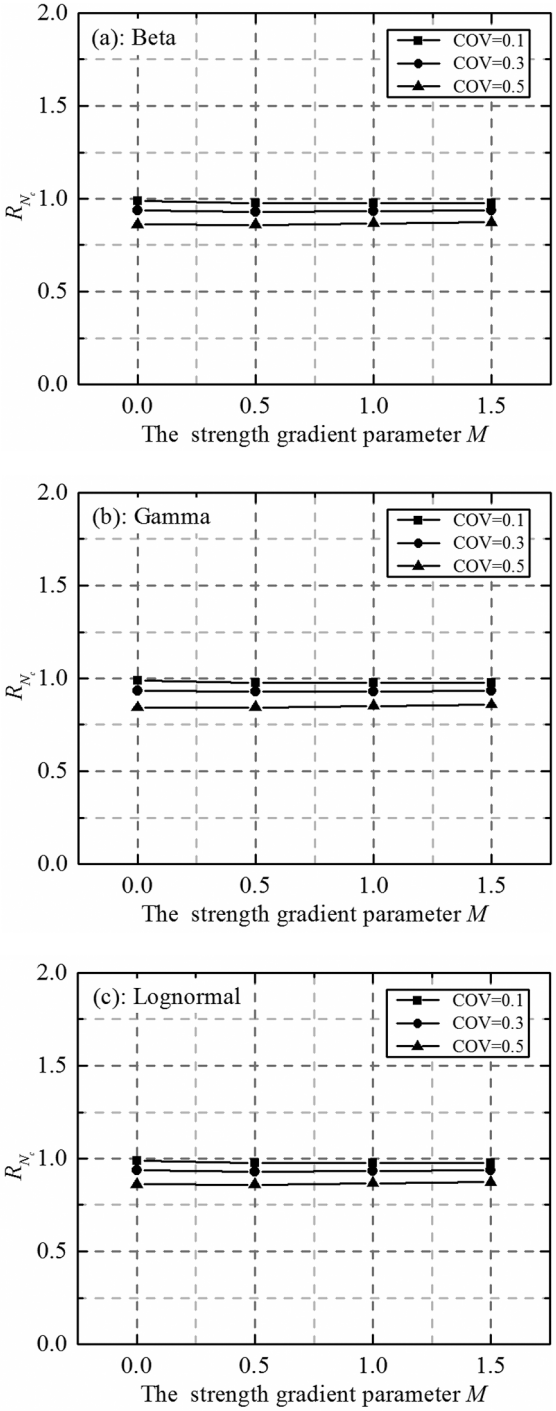

Fig. 5. R_{N_c} for $\delta_v = 1$. (a): Beta; (b):Gamma; (c): Lognormal.

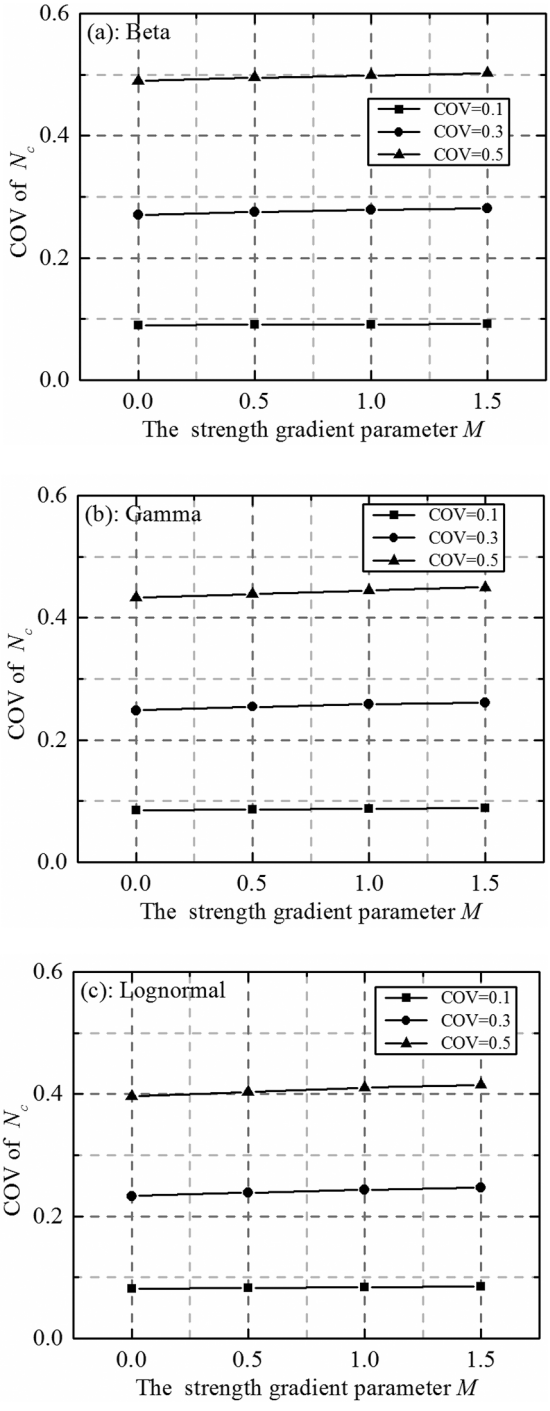

Fig. 6. The COV of the bearing capacity for $\delta_v = 1$. (a): Beta; (b):Gamma; (c): Lognormal.

strength gradient parameter M, distribution type, and vertical autocorrelation length are discussed. A series of computed results is shown in Figs. 3 and 4, which lead to the following observations concerning the influence of spatial variability of c_u of the foundation soil on the computed mean and standard deviation of bearing capacity:

(1) *effect of COV*: The estimated mean bearing capacity considering random field is smaller than the bearing capacity for deterministic analysis. As COV of c_u increases, the estimated mean bearing capacity decreases (as shown in Fig. 3(a)–(c)), while standard deviation of bearing capacity increases(as shown in Fig. 3(e)–(f)). Similar observation about the effect of COV of c_u on the estimated mean bearing capacity was firstly given by Griffiths and Fenton [12]. However, the influence of COV of c_u on the standard deviation of bearing capacity is more noticeable since an increase in the deviation of c_u results in a higher deviation of bearing capacity.

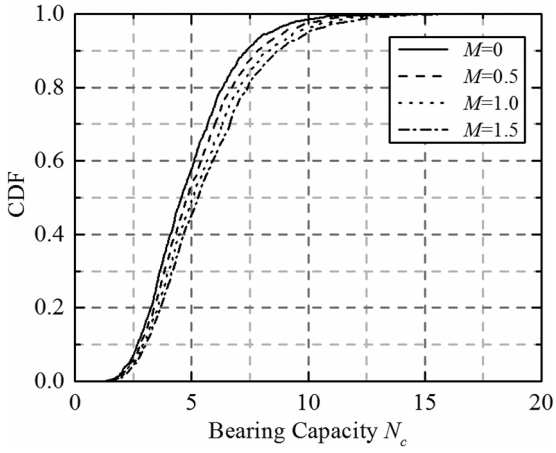

Fig. 7. The CDFs of the bearing capacity with lognormal distributed undrained shear strength, $\delta_v = 1$, and COV = 0.5.

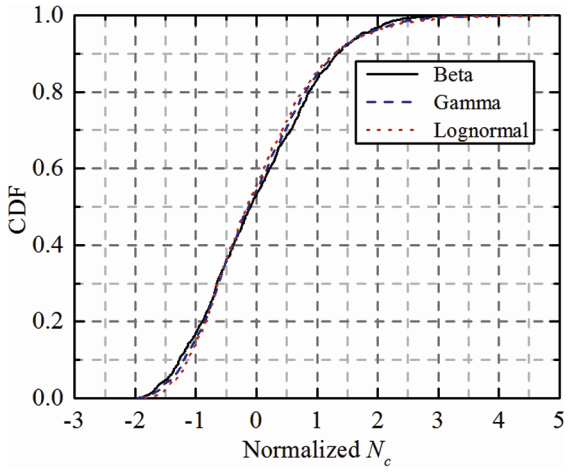

Fig. 8. The CDFs of the normalized bearing capacity with COV = 0.5, $\delta_v = 1$, and $M = 0$.

(2) *effect of M*: Both the mean and standard deviation of bearing capacity generally linearly increase with the strength gradient parameter *M*, which can be observed in all the subplots in Figs. 3 and 4. The difference between estimated mean bearing capacity considering random field and the bearing capacity for deterministic analysis does not show significant changes with the increasing of *M*. Specifically, for larger value of COV of c_u, standard deviation of bearing capacity increases steeply with *M*.

(3) *effect of distribution type*: It is obvious that the distribution type has an impact on the computed results of bearing capacity, even when they have the same mean and standard deviation. In particular, the effect of different distribution types is enlarged for larger COV of c_u. Furthermore, from Fig. 3(c) and (f), it is easily observed that Lognormal distribution shows the largest value in the estimated mean bearing capacity but smallest value in the corresponding standard deviation. This may due to reason that, for the Lognormal distribution, more values are distributed around the mean value of the random field.

(4) *effect of vertical autocorrelation length*: As Li et al. [21] pointed out, the effect of vertical autocorrelation length on the probabilistic results of bearing capacity is more significant for foundation soils with higher values of COV of c_u. It is by this consideration, the mean and standard deviation of bearing capacity for different cases of vertical autocorrelation length with COV = 0.5 are studied, results as shown in Fig. 4. Generally, both the mean and standard deviation of bearing capacity increase with the increase of the vertical autocorrelation length. Similar conclusions with respect to stationary random field case are drawn by Griffiths and Fenton [12], and by Li et al. [21] for non-stationary random field case.

Alternatively, the ratio between the estimated mean bearing capacity and the corresponding bearing capacity for the deterministic case is investigated. The ratio is defined as:

$$R_{N_c} = \frac{u_{N_c(M)}}{Det_{N_c(M)}} \tag{13}$$

where $u_{N_c(M)}$ is the estimated mean bearing capacity for a certain case with a strength gradient parameter *M*, $Det_{N_c(M)}$ is the bearing capacity of the deterministic analysis, in which c_u linearly increases over depth with a strength gradient parameter *M*. Note that, $Det_{N_c(M)}$, which is normalized by $u_{c_u(z=0)}$ (i.e. 40 kPa in this study), is also dimensionless.

Fig. 5 shows R_{N_c} in the analyzed cases. It was found that R_{N_c} changes slightly with the value of *M*, and may be considered as a constant value. Moreover, if COV of bearing capacity is investigated, similar results can be obtained as shown in Fig. 6. The COV of bearing capacity slightly increases with the value of *M*, but, to a certain extent, may also be considered as a constant value.

4.2. Statistical distribution characteristics of the bearing capacity

In this section, the statistical distribution characteristics of bearing capacity are studied. Fig. 7 shows some typical CDFs of bearing capacity for different values of *M*. These results indicate that the bearing capacity will be underestimated if a stationary random field model is considered. This conclusion seems to differ from that given by Li et al. [21], perhaps due to the different ways of normalizing the bearing capacity. For example, the bearing capacity is normalized by $u_{c_u(z=0)}$ in this study, while by $u_{c_u(z=5m)}$ (the mean c_u in the mid-depth) in Li et al. [21]. Interestingly, if the bearing capacities are normalized by the same way, the conclusions will agree with each other.

Furthermore, if the resulted bearing capacity for each case is normalized by:

$$\bar{N}_c(M) = \left(N_c(M) - \mu_{N_c(M)}\right)/\sigma_{N_c(M)} \tag{14}$$

where $\bar{N}_c(M)$ is the normalized N_c with zero mean value and unit variance for a certain case with a strength gradient parameter *M*; $\mu_{N_c(M)}$ and $\sigma_{N_c(M)}$ are the estimated mean and standard deviation of bearing capacity for the corresponding case.

Fig. 8 shows the CDFs of $\bar{N}_c$ for different distribution types, it was found that, different types of undrained shear strength lead to different shapes of CDFs of normalized N_c. Since both Lognormal and Gamma distributions have richer right tails than Beta distribution, the c_u with Lognormal or Gamma distribution produces a larger amount of higher bearing capacity than the c_u with Beta distribution.

When the CDFs of $\bar{N}_c$ for different values of *M* are compared, a very interesting phenomenon can be observed. If only *M* is different but other conditions defining the random field are the same, the CDFs of $\bar{N}_c$ for different values of *M* match each other very well (as shown in Fig. 9). This may due to the reason that, the soil is modeled by a linear-elastic perfectly plastic stress-strain law in this study. Furthermore, this good agreement in CDFs of bearing capacity can be utilized to predict the CDF of bearing capacity for non-stationary case according to the CDF of the corresponding stationary case as described in the following

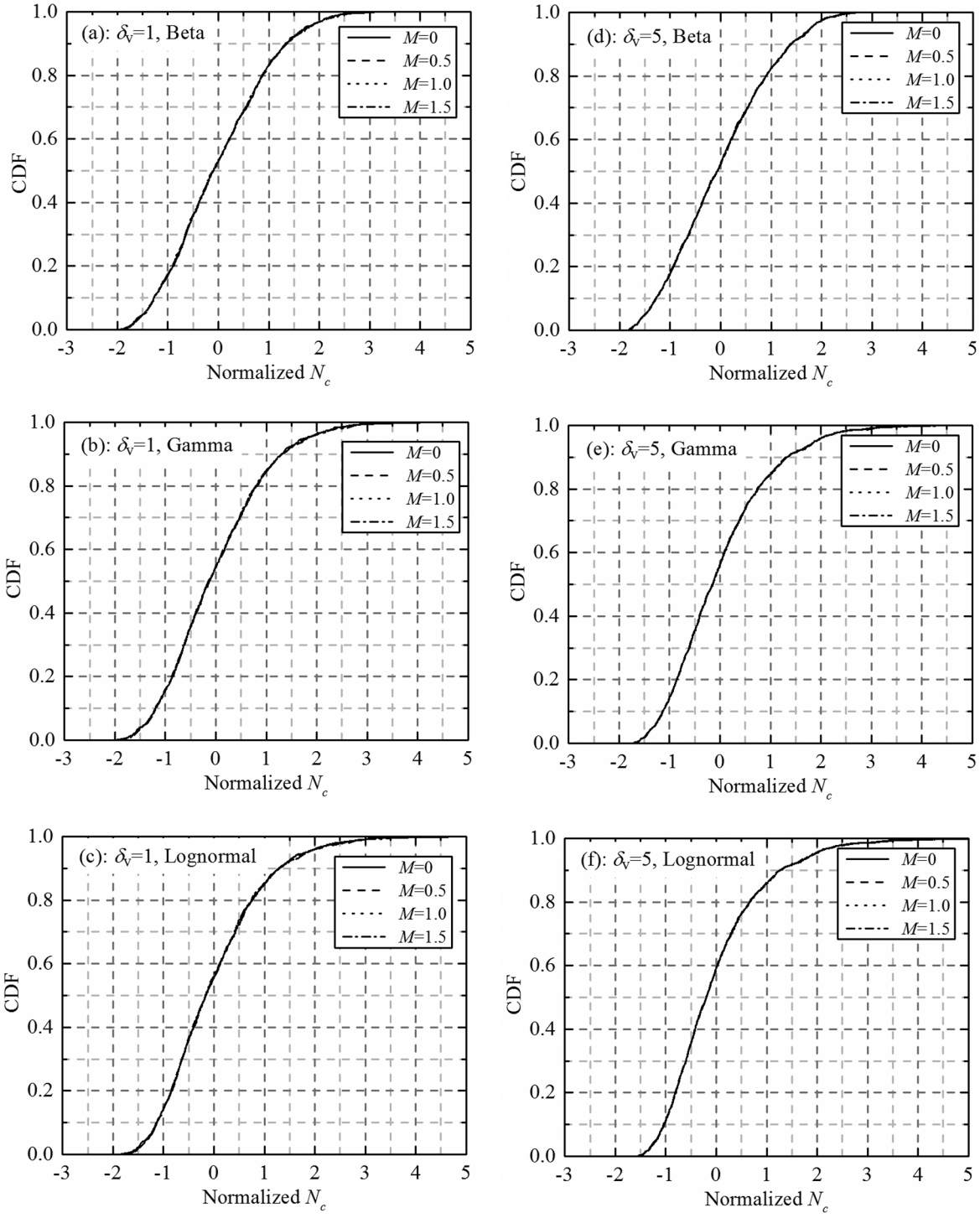

Fig. 9. The CDFs of the normalized bearing capacity with COV = 0.5. (a–c): δ_v = 1; (d–f): δ_v = 5.

section.

4.3. Predicting the CDFs of bearing capacity for non-stationary case utilizing the results of the corresponding stationary case

The benefit of estimating the CDFs of bearing capacity for the non-stationary case according to the result of the corresponding stationary case is obvious. To predict the stochastic characteristics of bearing capacity for the non-stationary case, firstly, the mean and standard deviation of bearing capacity for stationary case should be determined. As mentioned previously, two conclusions can be given:

(1) both the mean and standard deviation of bearing capacity linearly increases with *M*;

Table 3
Comparison of the mean and standard deviation of bearing capacity estimated by Scheme 1 and Scheme 2 with the target values.

	M	Mean					Standard deviation				
		Target	S1*	E1(%)*	S2*	E2(%)*	Target	S1	E1(%)	S2	E2(%)
Beta	0	4.637	–	–	–	–	2.271	–	–	–	–
	0.5	4.926	4.905	0.43	4.913	0.27	2.438	2.425	0.53	2.406	1.28
	1.0	5.192	5.173	0.37	5.123	1.32	2.591	2.579	0.46	2.509	3.12
	1.5	5.441	–	–	5.320	2.21	2.733	–	–	2.606	4.66
Gamma	0	4.762	–	–	–	–	2.059	–	–	–	–
	0.5	5.049	5.027	0.44	5.045	0.07	2.217	2.206	0.50	2.182	1.60
	1.0	5.312	5.292	0.38	5.261	0.96	2.362	2.353	0.38	2.275	3.71
	1.5	5.558	–	–	5.463	1.70	2.499	–	–	2.362	5.47
Lognormal	0	4.864	–	–	–	–	1.927	–	–	–	–
	0.5	5.149	5.128	0.41	5.153	−0.08	2.079	2.069	0.48	2.041	1.82
	1.0	5.410	5.392	0.33	5.373	0.69	2.220	2.211	0.41	2.128	4.09
	1.5	5.657	–	–	5.580	1.35	2.352	–	–	2.211	6.01

* S1 and S2 mean the value estimated by Scheme 1 and Scheme2, respectively. E1 and E2 are the relative error of Scheme 1 and Scheme 2, respectively.

(2) the ratio R_{N_c} and COV of bearing capacity can be considered as a constant value in the same case with different M.

According to these conclusions, two schemes can be proposed to estimate the mean value and standard deviation for different values of M. The first one (named as Scheme 1) is based on mean value and standard deviation of the stationary case ($M = 0$) and one non-stationary (i.e. $M = 1.5$), and the other one (named as Scheme 2) is only based on the mean value and standard deviation of the stationary case. Scheme 1 mainly utilizes the first conclusion to linearly interpolate the mean and standard deviation for any M, and Scheme 2 mainly utilizes the second conclusion according to the ratio and COV of bearing capacity in the stationary case as well as the deterministic result of bearing capacity for the corresponding non-stationary case.

The accuracies of those two schemes are shown in Table 3. It was found that, both the mean value and standard deviation can be well estimated by Scheme 1 since the relative error is around 0.5%, which is acceptable in geotechnical engineering. However, in Scheme 2, the relative errors of both the mean value and standard deviation increase with M. For small value of M (i.e. 0.5), the relative error of the mean value is lower than 0.5%, and the relative error of standard deviation is lower than 2%, while, for large value of M (i.e. 1.5), the relative errors of the mean value and standard deviation can reach 2% and 6%, respectively. The reason for the higher relative errors of standard deviation with respect to the large value of M is that, the COV of computed bearing capacity tends to increase slightly with M, while it is assumed as a constant in Scheme 2. By comparing the computational cost of these two schemes, Scheme 1 needs two sets of MCS for the case of $M = 0$ and $M = 1.5$, while Scheme 2 needs only one set of MCS for the case of $M = 0$ and one deterministic running for the corresponding M.

To predict the failure probability of strip footings, the CDFs of bearing capacity should be evaluated. There is no universal model to fit the PDF or CDF of bearing capacity for all different distributions of c_u. Therefore, it is desirable to utilize the estimated CDF of bearing capacity for stationary case to predict the CDF of bearing capacity for a certain non-stationary case. Since the CDF of normalized bearing capacity for different M matches each other very well, the CDF of bearing capacity for non-stationary case can be predicted according to the CDF of normalized bearing capacity for the stationary case as well as the corresponding mean value and standard deviation bearing capacity estimated by Scheme 1 and Scheme 2. Fig. 10 shows some typical results of the predicated CDFs based on Scheme 1 and Scheme 2. It is found that, for a lower M (i.e. $M = 0.5$), the difference between the CDF estimated by MCS (called the target CDF) and the CDFs predicated by Scheme 1 and Scheme 2 is insignificant. However, for a higher M (i.e. $M = 1.0$), the CDF predicated by Scheme 1 is also well identical with the target one, while the CDF predicated by Scheme 2 is slightly different from the target one. In all cases, the accuracy of these two schemes is deemed acceptable.

5. Summary and Conclusions

This paper focuses on investigating the stochastic result of bearing capacity in the presence of non-stationary spatially variable of c_u, which is modeled by a non-stationary random field with non-zero mean at the ground surface and linearly increased mean with depth, but a constant coefficient of variation. The spectral representation method was extended to simulate the non-stationary non-Gaussian random field, which, in turn, was applied to generate realizations of non-stationary random field with Beta, Gamma and Lognormal distributions. Then, MCSs were carried out to evaluate the statistical characteristics of the bearing capacity. Parametric studies were performed to investigate the effects of: (1) COV associated with the random field of c_u, (2) probability distribution function (PDF) of c_u, (3) the strength gradient parameter M defining the non-stationary feature of c_u; (4) vertical autocorrelation length. According to this study, the following conclusions were drawn:

(1) All the four factors as above mentioned have significant effects on the estimated mean and standard deviation of bearing capacity. In particular, both the estimated mean and standard deviation of bearing capacity increase linearly with strength gradient parameter M.
(2) The influence of M on $R_{N_c}$and COV of bearing capacity is very minimal. As a result, both R_{N_c} and COV of bearing capacity may be considered as constant values with different M.
(3) The CDFs of the normalized bearing capacity with different value of M match each other very well.

Last but not least, two computation schemes were introduced to predicate the mean and standard deviation, and even CDF of bearing capacity for any non-stationary random field of c_u, utilizing the results of the stationary case (sometimes with one more non-stationary case). The high accuracy of these two schemes was demonstrated through numerical examples.

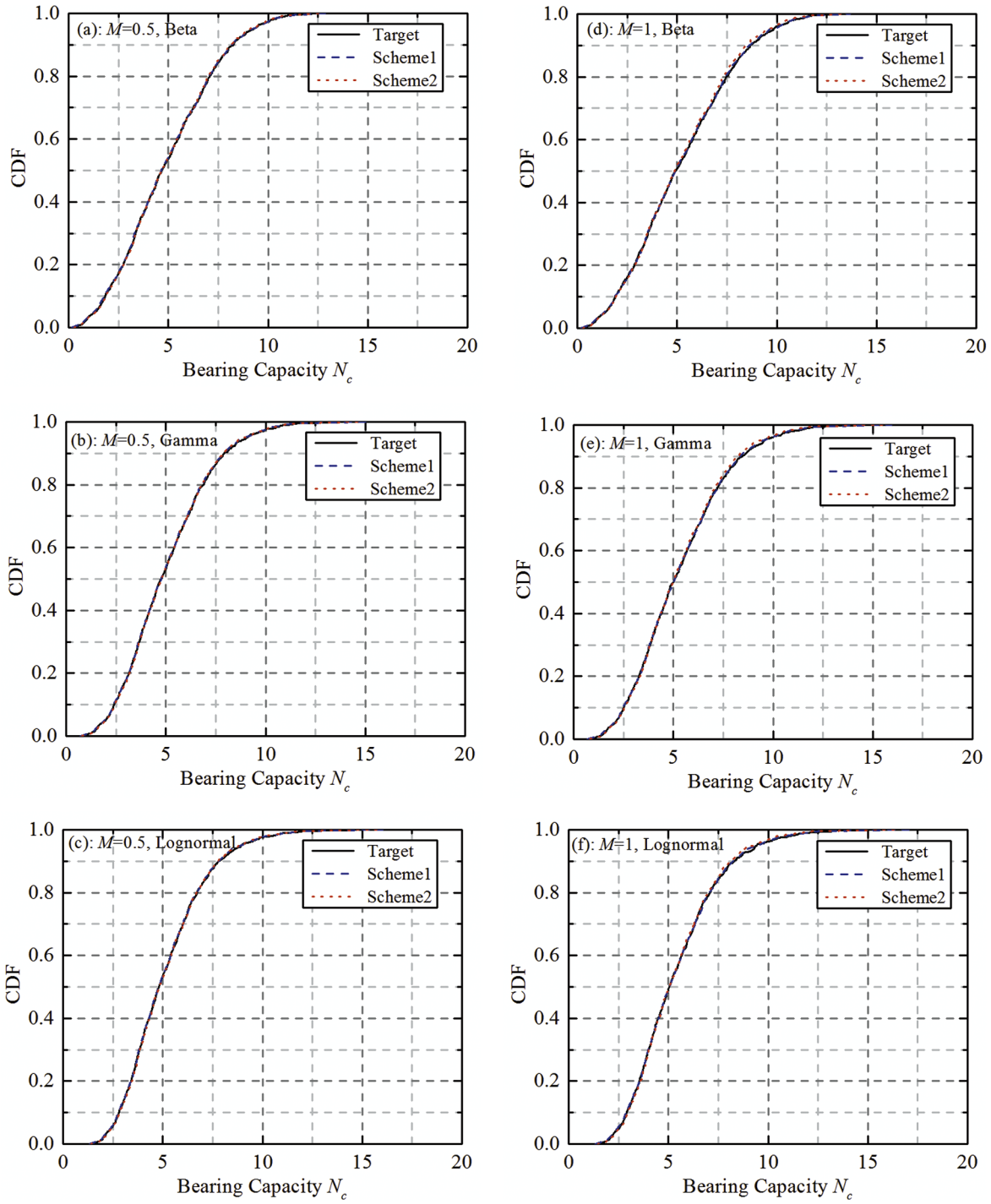

Fig. 10. Comparison of the CDF of the bearing capacity estimating by two schemes with the corresponding target one with $\delta_v = 1$, and COV = 0.5. (a–c): $M = 0.5$; (d–f): $M = 1.0$.

Acknowledgement

The supports by the National Natural Science Foundation of China (Grant No. 41630638), the National Key Basic Research Program of China (Grant No. 2015CB057901), the National Key Research and Development Program of China (Grant No. 2016YFC0800205), and the 111 project (No. B13024) are greatly acknowledged.

Appendix A

According to Wu et al. [36], the general steps of the iterative scheme to estimate the underlying Gaussian PSD function are simply described as follows.

Step 1: Give the underlying Gaussian PSD function

At the first step, an initial guess for the underlying Gaussian PSD function should be provided. Generally, the initial underlying Gaussian PSD function $S_G^{(0)}(\kappa_x, \kappa_z)$ can be assumed as the target non-Gaussian PSD function $S_{NG}^T(\kappa_x, \kappa_z)$.

Step 2: Compute non-Gaussian PSD function

At iteration (i), once a Gaussian PSD function $S_G^{(i)}(\kappa_x, \kappa_z)$ is given, the corresponding Gaussian autocorrelation function $\rho_G^{(i)}(\xi_x, \xi_z)$can be obtained through the two-dimensional Winner-Khinchine equation

$$\rho_G^{(i)}(\xi_x, \xi_z) = \int_{-\infty}^{+\infty}\int_{-\infty}^{+\infty} S_G^{(i)}(\kappa_x, \kappa_z) e^{i(\kappa_x\xi_x + \kappa_z\xi_z)} d\kappa_x d\kappa_z \tag{A1}$$

where superscript (i) indicates the i-th iteration of the algorithm.

The corresponding non-Gaussian autocorrelation function $\rho_{NG}^{(i)}(\xi_x, \xi_z)$can be determined from the above Gaussian autocorrelation function $\rho_G^{(i)}(\xi_x, \xi_z)$ through the translation field theory (shown in Eq. (8)). Then, the non-Gaussian PSD function $S_{NG}^{(i)}(\kappa_x, \kappa_z)$ is obtained by means of the inverse version of two-dimensional Wiener-Khintchine transform (shown in Eq. (9)).

Step 3: Decide whether the iteration goes on or not

After obtaining the non-Gaussian PSD function $S_{NG}^{(i)}(\kappa_x, \kappa_z)$, it needs to decide whether the iteration will be ended or not. Generally, the decision can be made based on the relative between the computed non-Gaussian PSD function $S_{NG}^{(i)}(\kappa_x, \kappa_z)$ and the target non-Gaussian PSD function $S_{NG}^T(\kappa_x, \kappa_z)$:

$$\varepsilon^{(i)} = \frac{\int_{-\infty}^{+\infty}\int_{-\infty}^{+\infty} |S_N^T(\kappa_x, \kappa_z) - S_N^{(i)}(\kappa_x, \kappa_z)| d\kappa_x d\kappa_z}{\int_{-\infty}^{+\infty}\int_{-\infty}^{+\infty} S_N^T(\kappa_x, \kappa_z) d\kappa_x d\kappa_z} \tag{A2}$$

If the error becomes small enough (e.g. less than 1%) or stabilizes to a certain value, the iteration can be finished and the current underlying Gaussian PSD function should be saved. Otherwise, the upgrading of the underlying Gaussian PSD function $S_{NG}^{(i)}(\kappa_1, \kappa_2)$ should be conducted (as described in the following step).

Step 4: Upgrade the underlying Gaussian PSD function

If the error is not within a tolerance value, the underlying Gaussian PSD function $S_{NG}^{(i)}(\kappa_x, \kappa_z)$ should be upgraded through the following scheme:

$$S_G^{(i+1)}(\kappa_x, \kappa_z) = \left[\frac{S_N^T(\kappa_x, \kappa_z)}{S_N^{(i)}(\kappa_x, \kappa_z)}\right]^\beta S_G^{(i)}(\kappa_x, \kappa_z) \tag{A3}$$

where β is a parameter to control the convergence rate.

After upgrading, a new Gaussian PSD function $S_G^{(i+1)}(\kappa_x, \kappa_z)$, which is positive definite, is obtained. However, the variance of the underlying Gaussian PSD function will be changed through the upgrading shown in Eq. (A3). Thus, the new Gaussian PSD function $S_G^{(i+1)}(\kappa_x, \kappa_z)$ should be normalized by:

$$S_G^{N(i+1)}(\kappa_x, \kappa_z) = \frac{S_G^{(i+1)}(\kappa_x, \kappa_z)}{\int_{-\infty}^{+\infty}\int_{-\infty}^{+\infty} S_G^{(i+1)}(\kappa_x, \kappa_z) d\kappa_x d\kappa_z} \tag{A4}$$

where the superscript ^{N} denotes the normalization.

References

[1] Babu GLS, Mukesh MD. Effect of soil variability on reliability of soil slopes. Géotechnique 2004;54(5):335–7.
[2] Cao ZJ, Wang Y. Bayesian model comparison and characterization of undrained shear strength. J Geotech Geoenviron Eng ASCE 2014;140(6):04014018.
[3] Cho SE, Park HC. Effect of spatial variability of cross-correlated soil properties on bearing capacity of strip footing. Int J Numer Analyt Methods Geomech 2010;34(1):1–26.
[4] Cho SE. Probabilistic assessment of slope stability that considers the spatial variability of soil properties. J Geotech Geoenviron Eng ASCE 2010;136(7):975–84.
[5] Der Kiureghian A, Ke JB. The stochastic finite element method in structural reliability. Probabilistic Eng Mech 1988;3(2):83–91.
[6] Fan H, Huang Q, Liang R. Reliability analysis of piles on spatially varying soils considering multiple failure modes. Compt Geotech 2014;57:97–104.
[7] Fenton G. Error evaluation of three random-field generators. J Eng Mech ASCE 1994;120(12):2478–97.
[8] Fenton GA, Griffiths DV. Probabilistic foundation settlement on spatially random soil. J Geotech Geoenviron Eng ASCE 2002;128(5):381–90.
[9] Fenton GA, Griffiths DV. Bearing-capacity prediction of spatially random c-ø soils. Can Geotech J 2003;40(1):54–65.
[10] Fenton GA, Griffiths DV. Three-dimensional probabilistic foundation settlement. J Geotech Geoenviron Eng ASCE 2005;131(2):232–9.
[11] Fenton GA, Vanmarcke EH. Simulation of random fields via local average subdivision. J Geotech Geoenviron Eng ASCE 1990;131(2):232–9.
[12] Griffiths DV, Fenton GA. Bearing capacity of spatially random soil: the undrained clay Prandtl problem revisited. Géotechnique 2001;51(4):351–9.
[13] Griffiths DV, Fenton GA, Manoharan N. Bearing capacity of rough rigid strip footing on cohesive soil: probabilistic study. J Geotech Geoenviron Eng ASCE 2002;128(9):743–55.
[14] Griffiths DV, Fenton GA. Probabilistic slope stability analysis by finite elements. J Geotech Geoenviron Eng ASCE 2004;130(5):507–18.
[15] Griffiths DV, Huang J, Fenton GA. Influence of spatial variability on slope reliability using 2-D random fields. J Geotech Geoenviron Eng ASCE 2009;135(10):1367–98.
[16] Griffiths DV, Yu X. Another look at the stability of slopes with linearly increasing undrained strength. Géotechnique 2015;65(10):1–7.
[17] Grigoriu M. Crossing of non-Gaussian translation process. J Eng Mech ASCE 1984;110(4):610–20.
[18] Jiang S, Li D, Zhang L, Zhou C. Slope reliability analysis considering spatially variable shear strength parameters using a non-intrusive stochastic finite element method. Eng Geol 2014;168(1):120–8.
[19] Jiang S, Li D, Cao Z, Zhou C, Phoon KK. Efficient system reliability analysis of slope stability in spatially variable soils using Monte Carlo simulation. J Geotech Geoenviron Eng ASCE 2015;141(2):04014096.
[20] Jimenez R, Sitar N. The importance of distribution types on finite element analyses of foundation settlement. Comput Geotech 2009;36(3):474–83.
[21] Li D, Qi X, Cao Z, Zhou W, Phoon KK, Zhou C. Reliability analysis of strip footing considering spatially variable undrained shear strength that linearly increases with depth. Soil Found 2015;55(4):866–80.
[22] Li D, Qi X, Phoon KK, Zhang L, Zhou C. Effect of spatially variable shear strength parameters with linearly increasing mean trend on reliability of infinite slopes. Struct Saf 2014;49:45–55.
[23] Li J, Tian Y, Cassidy MJ. Failure mechanism and bearing capacity of footings buried at various depths in spatially random soil. J Geotech Geoenviron Eng ASCE 2015;141(2):04014099.

[24] Matheron G. The intrinsic random functions and their applications. Adv Appl Probab 1973;5:439–68.
[25] Muller R, Larsson S, Spross J. Multivariate stability assessment during staged construction. Can Geotech J 2016;53(4):608–18.
[26] Lumb P. The variability of natural soils. Can Geotech J 1966;3(2):74–97.
[27] Phoon KK, Kulhawy FH. Characterization of geotechnical variability. Can Geotech J 1999;36(4):612–24.
[28] Phoon KK, Huang SP, Quek ST. Implementation of Karhunen-Loeve expansion for simulation using a wavelet-Galerkin scheme. Probabilistic Eng Mech 2002;17(3):293–303.
[29] Popescu R, Deodatis G, Nobahar A. Effects of random heterogeneity of soil properties on bearing capacity. Probabilistic Eng Mech 2005;20(4):324–41.
[30] Popescu R, Deodatis G, Prevost JH. Simulation of non-Gaussian homogeneous stochastic vector fields. Probabilistic Eng Mech 1998;13(1):1–13.
[31] Salgado R, Kim D. Reliability analysis of load and resistance factor design of slopes. J Geotech Geoenviron Eng ASCE 2014;140(1):57–73.
[32] Sivakumar Babu GL, Srivastava A, Murthy DSN. Reliability analysis of the bearing capacity of a shallow foundation resting on cohesive soil. Can Geotech J 2006;43(2):217–23.
[33] Srivastava A, Sivakumar Babu GL. Effect of soil variability on bearing capacity of clay and in slop stability problems. Eng Geol 2009;108(1-2):142–52.
[34] Stefanou G, Papadrakakis M. Assessment of spectral representation and Karhunen-Loeve expansion methods for the simulation of Gaussian stochastic fields. Comput Methods Appl Mech Eng 2007;196(21):2465–77.
[35] Wang Y, Zhao T, Cao Z. Site-specific probability distribution of geotechnical properties. Comput Geotech 2015;70:159–68.
[36] Wu Y, Li R, Gao Y, Zhang N, Zhang F. Simple and efficient method to simulate homogenous multidimensional non-Gaussian vector field by the spectral representation method. J Eng Mech ASCE 2017;143(12):06017016.
[37] Yaglom AM. An introduction to the theory of stationary random functions. Mineola, N.Y.: Dover; 1962.
[38] Zhu D, Griffiths DV, Huang J, Fenton GA. Probabilistic stability analyses of undrained slopes with linearly increasing mean strength. Géotechnique 2017;67(8):733–46.
[39] Zhang J, Huang HW, Phoon KK. Application of the kriging-based response surface method to the system reliability of soil slopes. J Geotech Geoenviron Eng ASCE 2013;139(4):651–5.